Scientific Research Publishing

Open Journal of Composite Materials, 2025, 15(3), 143-161
https://www.scirp.org/journal/ojcm
ISSN Online: 2164-5655
ISSN Print: 2164-5612

Influence of the Binder/Sand Ratio on the Performance of Geopolymer Mortar

Kouassi Jean Louis Badou*, Conand Honoré Kouakou, Brahiman Traore, Edjikémé Emeruwa

Laboratory of Soil, Water and Geomaterials Sciences, UFR-STRM, Félix Houphouët Boigny University, Abidjan, Ivory Coast
Email: *badoujeanlouis@live.fr

How to cite this paper: Badou, K.J.L., Kouakou, C.H., Traore, B. and Emeruwa, E. (2025) Influence of the Binder/Sand Ratio on the Performance of Geopolymer Mortar. *Open Journal of Composite Materials*, **15**, 143-161.
https://doi.org/10.4236/ojcm.2025.153008

Received: April 7, 2025
Accepted: July 20, 2025
Published: July 23, 2025

Abstract

Kaolinitic clay is the most sought-after natural source of aluminosilicate for the production of geopolymers, but it is found in large quantities in the Ivory Coast, but remains little exploited. Thus, this study was carried out to use these clays to produce geopolymer mortars as a substitute for Portland sand-cement. Its objective is to find the binder/sand ratio for the use of these materials in construction. It is in this context that local clay and sand were characterized by granulometric analysis, X-ray fluorescence and DRX (X-ray Diffraction). This clay, calcined at 750˚C, then mixed with an alkaline solution, gives a geopolymer binder. For this geopolymer binder, sand was incorporated according to binder/sand ratios of 0.4 to 1, and mortars were produced. After molding, heat treatment at 80˚C and curing at room temperature for 28 days, these mortars, which have become blocks, are mechanically tested. Their accessible porosity to water and their apparent density were also determined. The results indicate that the clay is made up of 80% kaolinite, to which muscovite and quartz are added. The compressive strength of the mortars increases from 19.11 to 27.09 MPa for ratios increasing from 0.4 to 0.7 and then decreases to 23.55 MPa, while the flexural strength values vary from 4.35 to 5.86 MPa. The measured accessible porosity to water is between 16.18% and 21.14% and the density is between 1.81 and 1.91 g/cm^3. Mortars based on geopolymer binder and sand with a B/S ratio of 0.7 have the highest mechanical strength values. They can therefore be used in construction in the same way as sand-cement concrete blocks. This will reduce cement consumption. This B/S ratio of 0.7 will therefore be retained for the rest of the work.

Keywords

Geopolymer, Kaolinite, Sand, Mortar, Portland Cement, Mechanical Resistance

1. Introduction

Geopolymers are materials made from aluminosilicate sources, cold-activated by a strong alkaline solution. Aluminosilicate sources are generally provided by kaolinite clay. Kaolinite clay is the most commonly used natural raw material for producing geopolymer materials. Authors have shown that kaolinite clay sites exist in Côte d'Ivoire [1] [2], but remain little exploited. These kaolinitic clays could therefore be used through geopolymers.

These materials are of growing interest because their manufacturing process consumes less energy and produces less CO_2 than that of Portland cement [3]. In addition, these materials have good mechanical resistance, which justifies their potential use in the construction sector. The gradual replacement of Portland cement by geopolymers would therefore be an ecological solution to the pollution problem linked to the massive use of hydraulic cement. Furthermore, the use of geopolymers in the construction sector involves the production of mortars, as is the case with Portland cement.

A mortar is a paste obtained by mixing a binder and sand in varying proportions. Some authors have been interested in composite geopolymers containing sand. Nana studied the synthesis, impact on microstructure and durability of geopolymer mortars based on metakaolin reinforced with quartz sand [4]. His results suggest that the incorporation of more than 50% by weight of fine quartz sand (especially 60%) brings an improvement in porosity and mechanical resistance, mainly. He explains these observations by the interactions between the geopolymer matrix and the sand grains. According to Burciaga-Diaz, who studied geopolymers containing a single rate of 30% quartz [5], He notes that large quartz particles observed have fulfilled their function as fillers in the material and may have trapped metakaolin, thus preventing its reaction. On the other hand, Furkan, who has also studied the properties of several composite geopolymers, states that in the case of using silica sand, the SiO_2 content increases and contributes to geopolymerization [6]. This justifies the mechanical properties of geopolymer mortars. Only the amount of sand added was 2.25 times higher than that of metakaolinite.

Thus, although the addition of quartz sand brings a great improvement in the mechanical and physical properties of geopolymer mortars, there seems to be a lack of studies on the optimal value of the Binder/Sand (B/S) ratio to develop geopolymer mortars with greater mechanical resistance.

This study, therefore, aims to determine the ideal B/S ratio for the production of geopolymer mortars intended for the construction sector and then to understand its effects on the microstructure of these materials. The first part of this work presents the materials and experimental methods. Then, in the second part, the results are presented and discussed.

2. Materials and Methods

2.1. Raw Materials

The raw materials used in this work are composed of clay, alluvial sand and acti-

vator solution.

The clay used was collected from Krindjabo, a locality located in the south-eastern region of Ivory Coast. The white rock collected was diluted in a large quantity of water, then passed through a 125 μm sieve to reduce the sandy fraction. After a week of decantation, the supernatant water is removed, and the remaining paste is dried in an oven for 24 hours at a temperature of 105˚C to obtain the dry matter. This dry matter then undergoes a heat treatment at 750˚C for 5 hours to transform it into metakaolin. This increases its reactivity towards the alkaline solution [7].

The alkaline activator solution was prepared from sodium hydroxide (NaOH) pellets, anhydrous sodium silicate (SiO_3Na_2) granules and demineralized water. To obtain the 12M activator solution [8], 30.65% sodium hydroxide and 6.13% sodium silicate (mass composition) were dissolved in 63.21% distilled water, and then the mixture was homogenized. The resulting solution was stored for at least 24 hours before use.

Alluvial sand is of granular class 0/2. This sand is commonly used in Ivory Coast for building construction. It is commercially available and commonly used to make cement mortars. This sand was oven-dried for 24 hours at a temperature of 105˚C before use.

2.2. Development Method

The mortars were produced in several stages, which are summarized in **Figure 1**. First, the binder consisting of the alkaline activator solution and metakaolin is obtained by mixing them in an electric mixer of the COPLAIN BT 05 CS type, for 15 minutes, in a mass ratio of 1:1. Then, the quantity of sand corresponding to each formulation is added to the binder and the whole is mixed for about fifteen minutes. The mixture obtained is shaped into prismatic molds of dimensions 4 × 4 × 16 cm^3, as is the pasty binder obtained previously. Finally, in order to allow better setting of the test pieces, the prismatic molds containing the different mixtures are stored in a room at an average temperature of 27˚C and a relative humidity of 40% for 24 hours [9]. Subsequently, for the thermal activation of the geopolymerization reaction, the molds are placed in an oven controlled by a digital thermostat STC-1000 at a temperature of 80˚C [10] for 5 hours, as opposed to the 3 hours indicated by Liew in his review [11]. At the end of the 5 hours of thermal activation, the specimens are left to mature for 27 days under laboratory conditions (T = 27˚C; RH = 40%). After maturation (*i.e.*, at 28 days of age), the hardened specimens are subjected to characterization tests. **Table 1** gives the different formulations produced as well as the indices used to identify the different specimens.

Table 1. Table of indices and formulations.

Hint	B/S ratio	Metakaolinite/alkaline solution ratio
GB	-	1:1
GM0.4	0.4	1:1

Continued

GM0.5	**0.5**	**1:1**
GM0.6	0.6	1:1
GM0.7	0.7	1:1
GM0.8	0.8	1:1
GM0.9	0.9	1:1
GM1	1	1:1

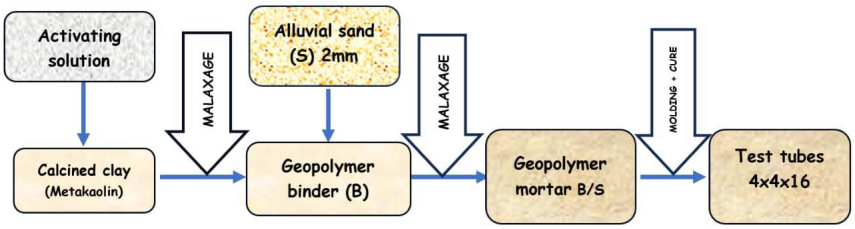

Figure 1. Schematic diagram of the synthesis of geopolymer mortars.

2.3. Characterization Techniques

2.3.1. Tests on the Raw Material

Raw clay and calcined clay from Krindjabo were subjected to chemical, mineralogical and microstructural characterization tests to determine their suitability for the development of geopolymers.

The chemical composition of the clay was obtained using an OXFORD X-Supreme 8000 X-ray fluorescence spectrometer according to the method of ASTM E1621-13 standard [12]. The results are presented in a table as a percentage by mass of oxide.

The mineralogical analysis was carried out using a BRUKER-AXS (SIEMENS) D5005 X-ray diffractometer using Cu Kα radiation (λKα = 1.54056 Å, 40 kV/35mA). It allowed obtaining a spectrum from which the main peaks on the diffractogram of the different mineralogical phases were indexed using the mineralogical analysis software "MATCH!" and "PROFEX" by comparison with the JCPDS (Joint Committee on Powder Diffraction Standards) files of the ICDD (International Centre for Diffraction Data). Then the respective proportions (the mineralogical composition) of these different phases are calculated as a percentage according to the NF EN 13925-1 method [13]. The microstructural characterization of the clay was carried out with a scanning electron microscope type HIROX SM-4000 M at 15 kV.

The granulometry of the alluvial sand used during this study was determined by sieving using a RETSCH AS 200 laboratory sieve. The sample was prepared according to the requirements of the French standard NF EN 933-1 [14]. The test lasts 3 minutes.

2.3.2. Test on Geopolymer Mortars

The open porosity accessible to water and the absolute density of the produced

materials were determined by the hydrostatic weighing method on geopolymer mortar specimens according to the French standard NF P18-459 [15]. The masses in water (M_{water}), wet mass in air (M_{air}) and the dry mass at 105˚C (M_{dry}) of the specimen were measured. The apparent density (d) and the open porosity to water (ε) were calculated respectively from the following formulas:

$$d = \frac{M_{dry}}{M_{air} - M_{water}} \tag{1}$$

and

$$\varepsilon(\%) = \frac{M_{air} - M_{dry}}{M_{air} - M_{water}} \times 100\% \tag{2}$$

The MATEST E181N compression and bending machine (300/15 kN), controlled by a CYBER-PLUS PROGRESS control unit, was used to carry out bending and compression tests on specimens in accordance with the French standard NF EN 196-1 [16]. The values of flexural strength (R_f) and compressive strength (R_c) for the different specimens were calculated using the formulas from the measured values of the breaking loads (F):

$$R_f = \frac{3F \cdot l}{2b \cdot h^2} \tag{3}$$

and

$$R_c = \frac{F}{b^2} \tag{4}$$

with:

F: the breaking load in bending or compression of the specimen (N);

l: the distance between the supports (mm);

b and h: the width and height of the test piece (mm).

Fourier transform infrared spectroscopy made it possible to identify the characteristic bonds in the geopolymer mortar and to assess the different chemical transformations of the clay. A spectrum is plotted from the measurements made with a Jasco FTIR 4600 TYPE A spectrometer in transmission mode [17].

3. Results

3.1. Characteristics of Raw Materials

3.1.1. Characteristics of Sand

The sand granulometric analysis curve is shown in **Figure 2**. This allowed us to determine the granulometric parameters of the sand studied in accordance with the French standard NF EN 933-1. This sand is composed of 36% fine sand (80 µm - 300 µm), and 56% medium sand (300 µm - 1.2 mm). Its fine particle content (<0.08 mm) is 2% while that of coarse sand is 6% (>1.25 mm). Its granular class is therefore 0/2, *i.e.*, the grains have a size between 2 µm and 2 mm. The median diameter of the sand (D50 value) is equal to 0.40 mm. The uniformity coefficient (Cu) being equal to 3.2, the granulometry of the sand is therefore spread. This means that this sand is composed of a wide variety of particle sizes. The value of

the curvature coefficient is equal to 0.86; this sand is therefore poorly graded, because the Cc is less than 1, which is confirmed by its predominance of fine and medium sand.

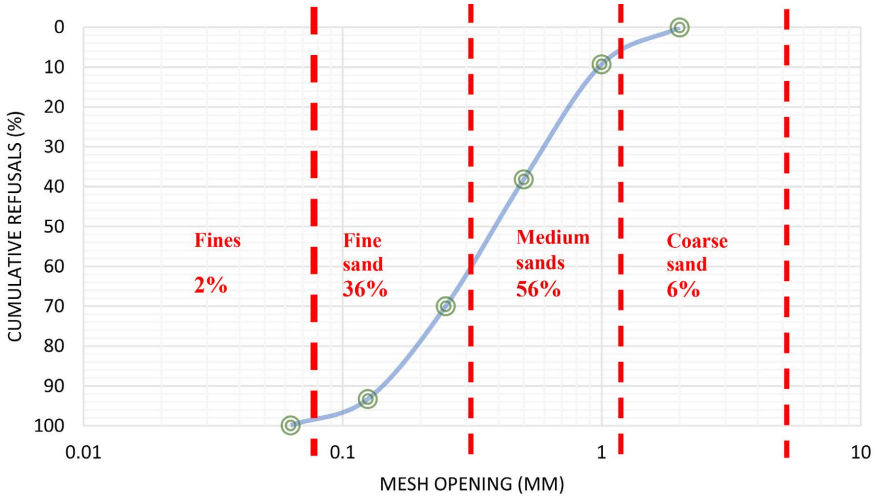

Figure 2. Granulometric curve of alluvial sand.

3.1.2. Characteristics of Clay

Chemical analysis made it possible to identify and quantify the major oxides of Krindjabo clay (Table 2). Silica (SiO_2) and alumina (Al_2O_3) are the major oxides with a mass proportion of 55.95% and 38.47% respectively. Its SiO_2/Al_2O_3 ratio is equal to 1.45 while in the case of pure kaolinite, this ratio is 1.17 [18]. This clay therefore contains free silica in the form of quartz grains. Potassium oxide (K_2O), titanium oxide (TiO_2), calcium oxide (CaO), and sodium oxide (Na_2O) have contents of less than 1%. The other unidentified oxides have a total content of 3.1%. For comparison, only the Anguédédou clay has a SiO_2/Al_2O_3 ratio of less than 1.45 (Table 3). It therefore contains less free silica than the Krindjabo clay. The content of coloring oxides (Fe_2O_3 and TiO_2) is relatively low (<2%), which explains the very white color of the clay. Meanwhile, clays collected from other sites in Côte d'Ivoire have iron oxide levels between 2.90% and 6.72% (Table 3).

Table 2. Mass composition of major oxides in Krindjabo clay.

Oxides	SiO_2	Al_2O_3	Fe_2O_3	K_2O	TiO_2	CaO	Na_2O	Others
Mass content %	55.91	38.47	0.91	0.89	0.57	0.05	0.1	3.1

Table 3. Mass composition of major oxides in some clays from Ivory Coast.

Oxides	SiO_2	Al_2O_3	Fe_2O_3	TiO_2	Na_2O	K_2O	CaO	MgO	P_2O_5	MnO	SO_3	ZrO_2	Cr_2O_3	SrO
Bingerville	54.70	36.80	5.32	1.18	0.29	1.26	0.02	0.26	0.10	0.05	0.17	0.96	0.06	-
Anyama	59.85	27.15	6.72	0.03	1.25	3.41	0.03	0.29	0.12	0.03	0.28	0.03	0.67	-
Dabou	56.20	27.75	6.60	1.19	0.64	1.79	1.14	0.73	0.10	0.07	1.19	0.86	0.06	-
Anguédédou	53.90	39.80	2.90	2.87	<0.01	0.44	0.04	<0.19	<0.37	-	<0.20	0.10	0.74	0.02
Aleppo	60.60	32.50	3.47	0.78	<0.01	3.51	<0.12	0.85	<0.01	-	<0.14	0.03	0.67	<0.01

The main peaks at angles 12.23˚, 20.31˚ and 24.78˚ on the diffractogram (Figure 3) are attributed to kaolinite. The peaks at angles 8.80˚, 17.68˚ and 19.87˚ are related to muscovite. Quartz is identified by the peaks at 20.80˚, 26.56˚, and 36.48˚. The peaks at 24.26˚, 33.30˚ and 35.81˚ indicate the presence of hematite. In addition, Table 4 gives the approximate mass proportions of these different minerals identified using the "MATCH!" and "PROFEX" software. The main mineral in this clay is kaolinite with a mass content of 88.29%, muscovite is also present with 10.58%, quartz (free silica) has a content of 1.01% and the hematite rate is 0.1%. These proportions can also be calculated from the results of chemical analysis using the method proposed by Bich [19]. The results given by the Bich method are slightly different from those of the method used here, because it relies on a virtual chemical composition of the minerals.

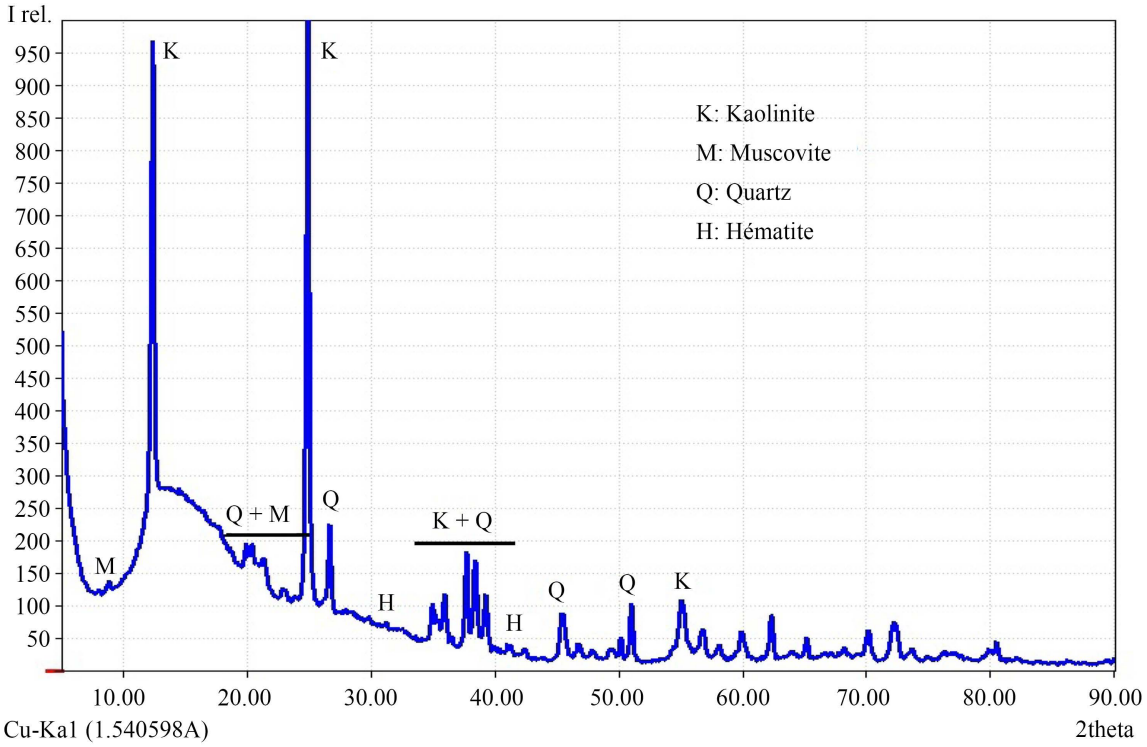

Figure 3. Diffractogram of raw clay.

Table 4. Mineralogical composition of raw clay.

Mineral	Kaolinite	Muscovite	Quartz	Hematite
Mass content %	88.29	10.58	1.01	0.1

Scanning electron microscopy of this clay (Figure 4(a)) shows irregularly shaped sheet-like clay particles scattered among silica grains of a few microns in size. This suggests that the kaolinite in this clay is poorly crystallized. Figure 4(b) shows that the calcined clay has virtually no sheet-like particles, confirming its transformation into metakaolin.

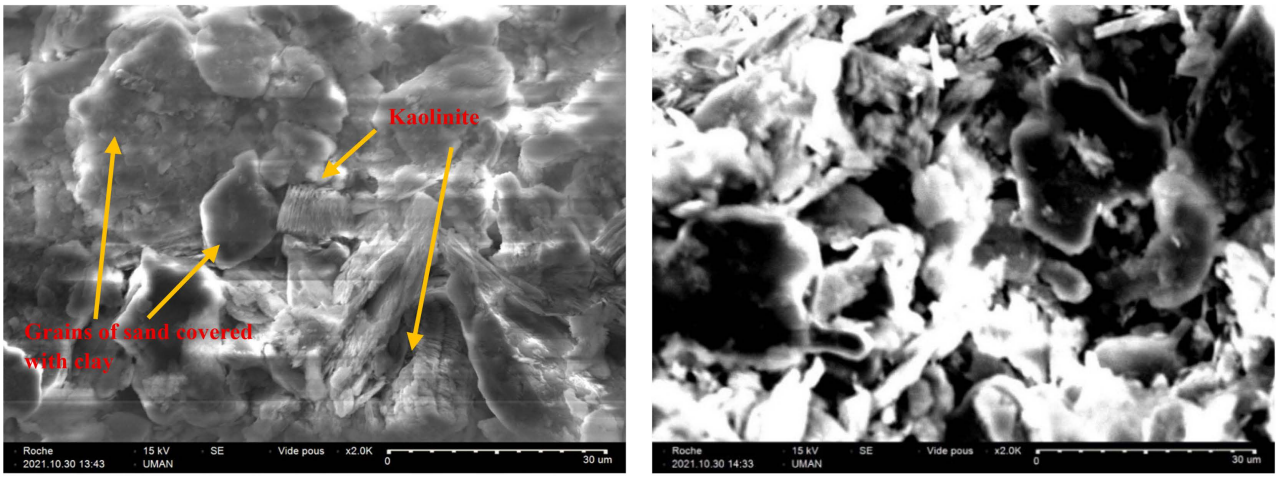

(a) (b)

Figure 4. (a) SEM image of natural clay; (b) SEM image of calcined clay.

3.2. Properties of Geopolymer Materials

3.2.1. Apparent Density

Figure 5 shows the evolution of the density of mortars according to the values of the B/S ratio after 28 days of conservation. The densities decrease linearly between 1.91 and 1.81 when the B/S ratio increases from 0.4 to 1 (the sand content then decreases from 71.43% to 50%). Overall, the density values obtained in this study are close to those of the mortars studied by some authors, which are between 1.9 and 2.2 [4] [20].

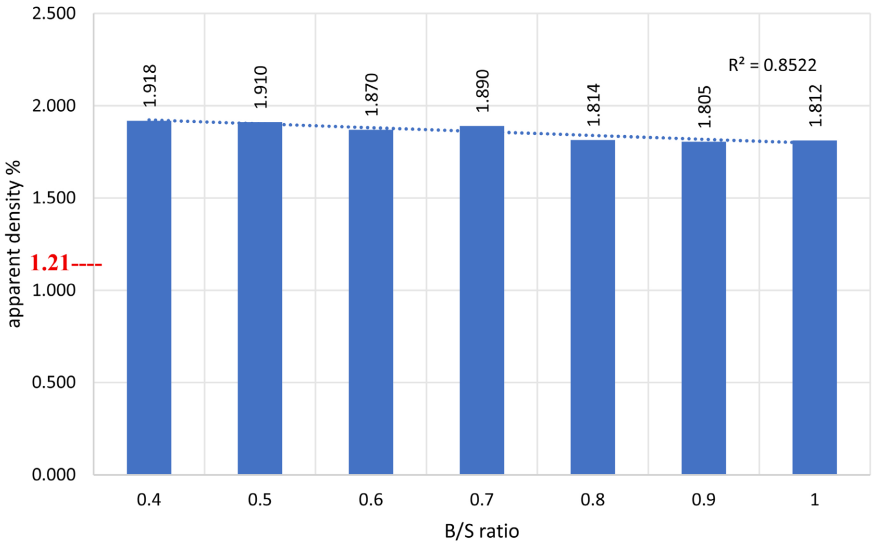

Figure 5. Apparent density of specimens as a function of the B/S ratio.

For the geopolymer binder (GB), the density is 1.21. On the other hand, geopolymer binders containing sand have higher densities, and the apparent density of sand is between 1.87 and 1.89. This increase in the density of the geopolymer

material is therefore due to the higher apparent density of the sand, between 1.5 and 1.8 [21]. The density of geopolymer mortar evolves in the same direction as the sand content. The more sand there is in the mortar (lower B/S ratio), the denser the mortar. The density of geopolymer mortar could therefore be presented as a function of the proportion of sand and that of metakaolin [22]. This decrease in density with the B/S ratio could be linked to the presence of pores in the geopolymer matrix.

3.2.2. Porosity Accessible to Water

The results of the water accessible porosity are shown in the graph in **Figure 6**. The graph shows the evolution of the porosity of geopolymer mortars as a function of the B/S ratio. Without sand, the geopolymer binder (GB) has a water accessible porosity of 43.18%, a value greater than 20%; the geopolymer binder is therefore a porous material [23]. The porosity of geopolymer mortars varies between 20.14% and 16.17%, which is lower than that of the geopolymer binder. The presence of sand in the mortars leads to a reduction in their porosity.

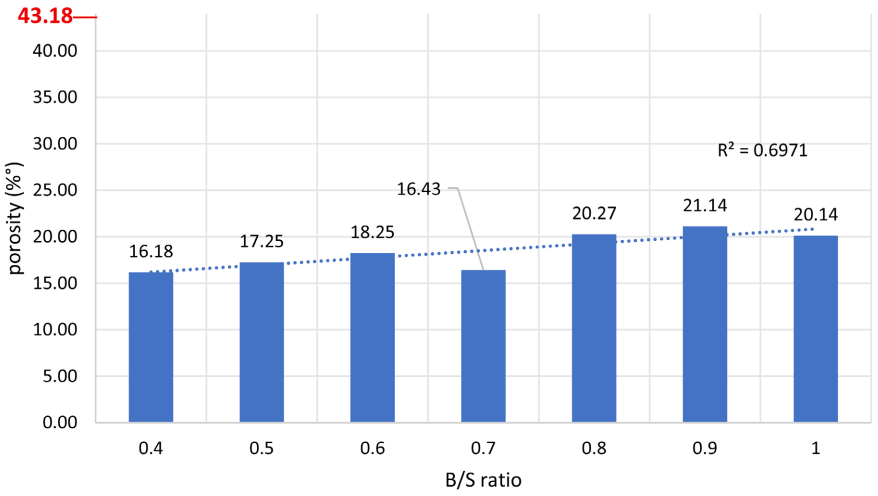

Figure 6. Water-accessible porosity of geopolymer mortar specimens according to B/S ratios.

Generally, when the B/S ratio increases, *i.e.*, the amount of sand decreases, the porosity accessible to water is high. On the other hand, when this B/S ratio decreases, the amount of sand increases, and the porosity decreases. Thus, for B/S ratios ranging from 1 to 0.4, the porosity decreases from 20.14% to 16.17%. These results are similar to those obtained by Nana *et al.* (**Table 5**).

Table 5. Comparison of the results of this study and those of Nana *et al.*

	B/S ratio	Sand content (%)	Apparent porosity (%)
Result of this study	1	50	20.13
	0.6	62.5	18.25

Continued

Nana *et al.* (2020)	1	50	20.75
	0.66	60	18.32

These water-accessible porosity values have an impact on the mechanical properties of geopolymer mortars.

3.2.3. Mechanical Resistances

The results of mechanical tests (flexural strength and compressive strength) carried out on geopolymer mortar specimens of different B/S ratios are given in Figure 7. The geopolymer binder has a compressive strength of 19.08 MPa and a flexural strength of 3.89 MPa.

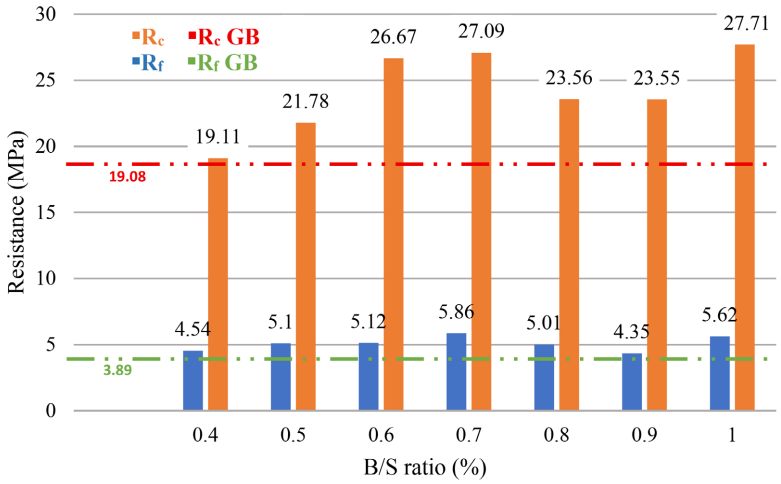

Figure 7. Mechanical resistance of geopolymer mortars: R_c (compressive strength), R_f (flexural strength), R_c and R_f of geopolymer binder (GB).

The flexural and compressive strengths of geopolymer mortars, for B/S ratios between 0.4 and 0.7, vary from 4.54 to 5.86 MPa and from 19.11 MPa to 27.09 MPa respectively. While for B/S ratios between 0.7 and 0.9, the flexural and compressive strengths of geopolymer mortars vary from 5.86 MPa to 4.35 MPa and from 27.09 MPa to 23.55 MPa respectively, to undergo a slight increase when B/S is equal to 1. However, the increase in the strength values, for B/S ratios ranging from 0.4 to 0.7, seems to be accompanied by a decrease in density and an increase in porosity. Whereas beyond the B/S ratio equal to 0.7, the variation in resistance appears to be caused by the decrease in density and the increase in porosity of the specimens.

Variations in strength with density and porosity are induced by the reduction in the amount of sand in mortars and the structuring of the different mixtures. Indeed, with the reduction in the amount of sand, the compactness decreases due to the greater proportion of geopolymer binder. This promotes the coating of the sand grains by the geopolymer binder but leads to a decrease in mechanical strength.

Furthermore, the B/S ratio equal to 0.7 therefore appears to be the optimal ratio for obtaining geopolymer mortars with greater mechanical resistance. However, the compressive strength values (27.09 MPa) are relatively lower than those of Portland cement mortars (32.5 MPa). The value of 32.5 MPa is used to characterize Portland cement. Regarding concrete blocks made from sand-cement mortar used in masonry, the NF EN 771-3/CN standard [24] recommends a compressive strength of 4 MPa for the assembly of partitions and 8 MPa for load-bearing walls. The GM0.7 geopolymer mortar, which has a mechanical resistance higher than that of raw earth bricks and fired bricks, can therefore be used for the production of concrete blocks for load-bearing or non-load-bearing walls. Indeed, according to the XP P 13-901 standard, the raw earth bricks (compressed) used in construction vary from 2 to 6 MPa [25], while the Eurocode 6 NF EN 1996 standard recommends resistance values between 2.8 and 11 MPa for fired bricks [26].

Furthermore, the B/S ratio equal to 0.7 corresponds to a percentage of sand in the geopolymer mortar equal to 58.82%. This percentage is close to that obtained by Nana *et al.*, who concluded at the end of their study that the addition of 60% quartz sand allows for the best mechanical resistance. Similarly, Kuenzel *et al.* obtained the best mechanical resistance for mortars prepared with 60% sand.

These mechanical properties could be related to the microstructure and chemical structure of geopolymer mortars.

3.3. Effects of the Binder/Sand (B/S) Ratio

3.3.1. Microstructure

In **Figures 8(a)-(c)**, the SEM photographs show the changes undergone by the raw materials. These changes are perceptible at the microscopic scale in the geopolymer matrix and on the sand grains. **Figure 8(a)** shows that the geopolymer binder (GB) (corresponding to a sample containing no sand) does not appear as a gel, as is the case for geopolymers based on blast furnace slag, but appears to be an agglomeration of clay particles [27]. The dissolution of metakaolin, therefore, does not appear to be complete, as shown by the work of certain authors, including Jaya [28]. The black dots visible on the surface indicate the presence of macropores (>50 nm) in the geopolymer binder, which allows a qualitative assessment of its porosity accessible to water [29].

In **Figure 8(b)**, the geopolymer mortar shows sand grains disseminated and embedded in the geopolymer matrix. However, discontinuities are visible at the sand grain-geopolymer matrix interface as shown by the enlargement of the sand-geopolymer binder interface in **Figure 8(c)**. This seems to justify the relatively low compressive strength values compared to those obtained by other authors, such as Wan *et al.* and Nana *et al.* Indeed, they obtained compressive strengths greater than 50 MPa, and the microstructure shows a good bond between sand grains and the geopolymer matrix. To confirm the transformation of the clay under the action of the alkaline solution, the mineralogical composition of the geopolymer binder and that of a geopolymer mortar were analyzed.

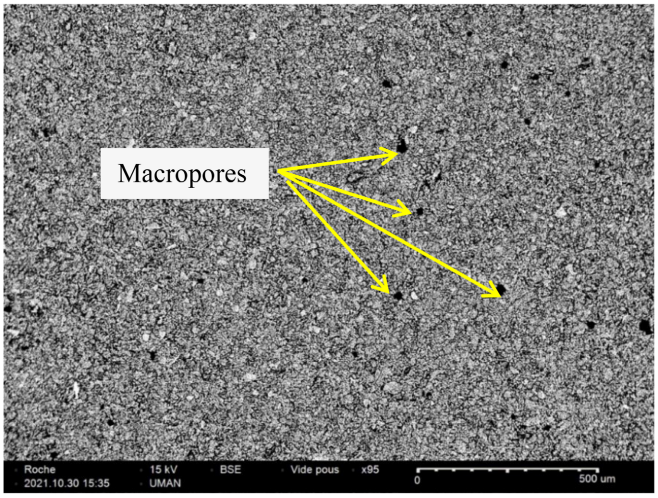

(a)

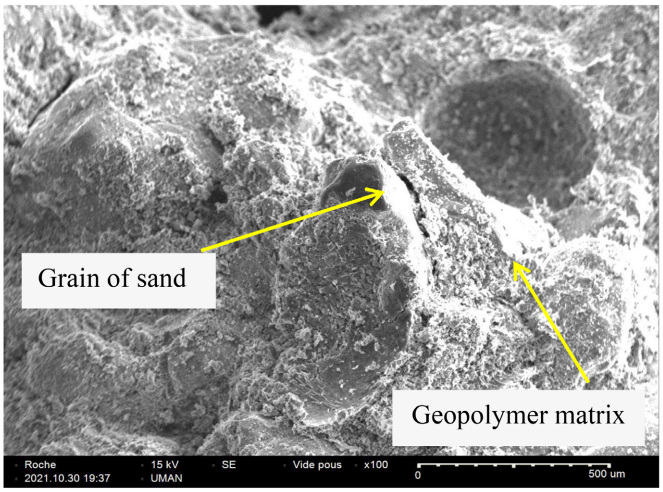

(b)

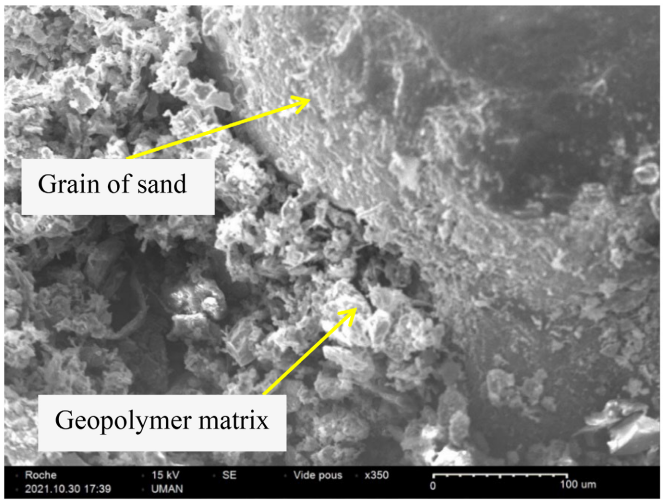

(c)

Figure 8. (a) Geopolymer binder; (b) geopolymer mortar; (c) zoom of the sand-geopolymer binder interface.

3.3.2. Mineralogical Composition

The superposition of the diffractograms of the raw clay, the geopolymer binder and a geopolymer mortar in Figure 9 shows that the peaks characterize the presence of kaolinite, quartz and muscovite. Comparison of these peaks on these different spectra shows that the peaks of kaolinite disappear on those of the geopolymer binder and the geopolymer mortar. This absence of peaks specific to kaolinite follows its transformation into metakaolin during the calcination of the clay at 750˚C. On the other hand, the only mineral phase that remains present on the spectra of the geopolymers (binder and mortar) is quartz, the main constituent of sand. Therefore, no new mineral phases appear after the action of the alkaline solution on the calcined clay. Thanks to the amorphous nature of metakaolin, the alkaline solution was able to act on the chemical structure of this precursor. To understand the transformations of the chemical structure of clay and sand minerals in the presence of soda and sodium silicate, the specimens of binder and geopolymer mortar were analyzed by infrared spectrometry (FTIR).

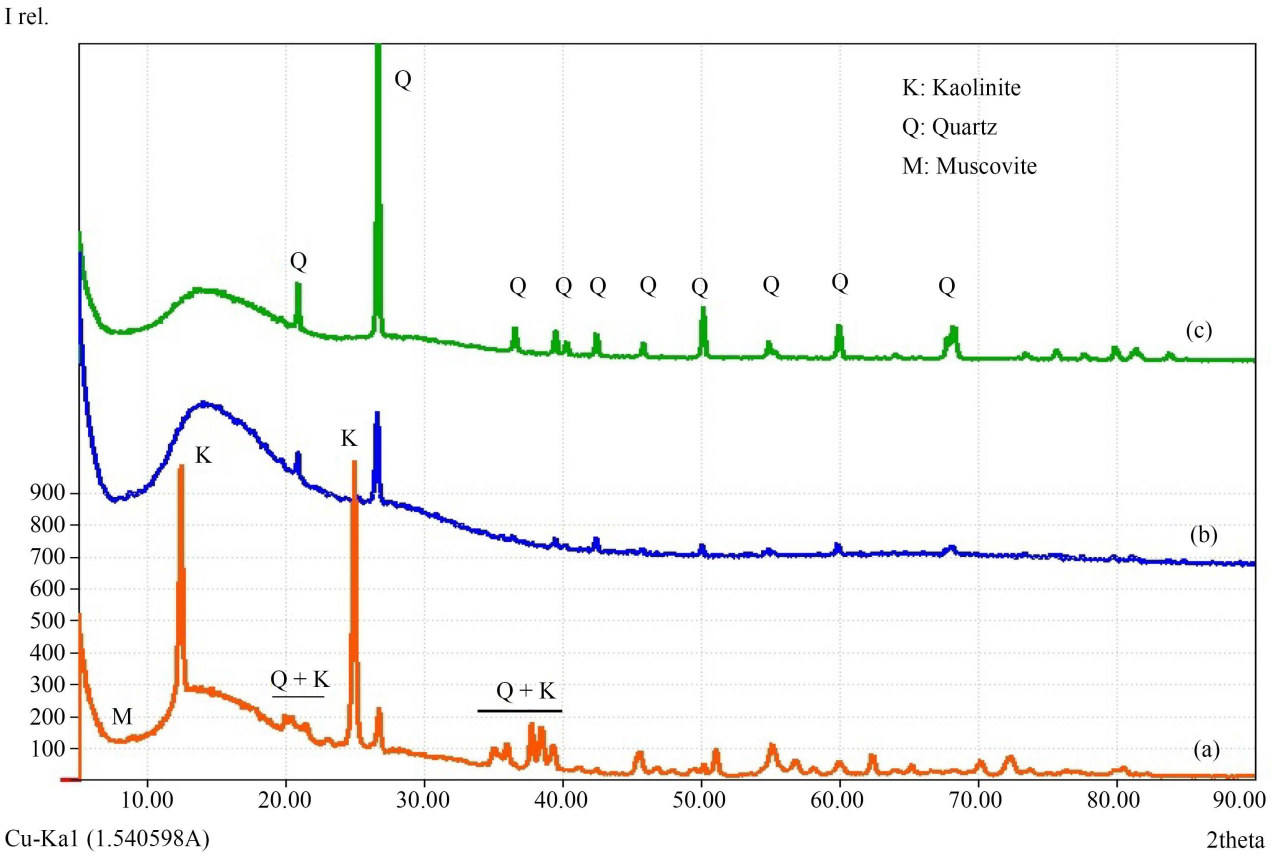

Figure 9. Diffractogram of: (a) raw clay; (b) geopolymer binder; (c) geopolymer mortar.

3.3.3. Chemical Structure

The infrared spectra of geopolymer binder (GB) and geopolymer mortars (GM) (Figure 10) show the evolution of the characteristic bonds of geopolymer binder and geopolymer mortars. The peaks in the band around 970.1 cm^{-1} attributed to

Si-O-Al and Si-O-Si bonds [30] [31], characteristics of geopolymer materials (poly(sialate-siloxo)) based on metakaolin, increase in intensity according to the binder/sand ratios. Indeed, for the geopolymer binder GB, this band has the lowest intensity, probably because of the low contribution of the Si-O-Al and Si-O-Si bonds present in the kaolinite of the clay. The geopolymer mortars GM1-GM0.9-GM0.7 and GM0.4 present more intense peaks in the 970.1 cm^{-1} band, certainly due to the presence of sand added to the geopolymer binder (GB). These observations could be explained by the conclusions of the study of some authors, in particular Lucas *et al.* Indeed, according to the results of his work, the sand undergoes a dissolution-reprecipitation before consolidating under the action of the alkaline solution prepared from soda and sodium silicate [32]. The possibility of dissolution of quartz sand is also mentioned in the study of Niibori, who used a concentrated NaOH solution to determine the dissolution rate of silica [33]. This therefore assumes a greater production of Si-O-Si type bonds in the chemical structure of mortars.

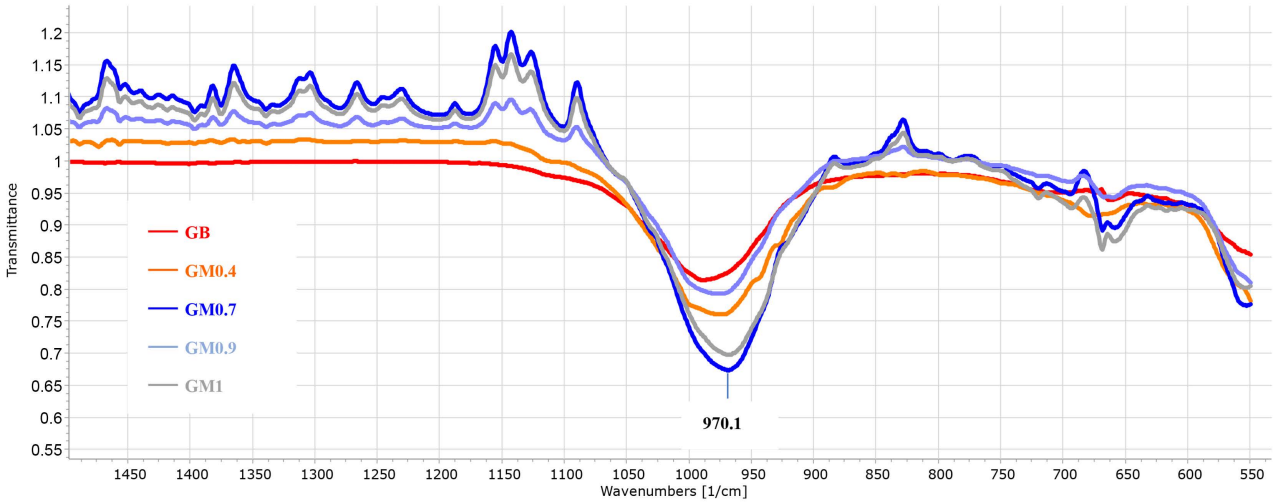

Figure 10. Infrared spectrum of geopolymer binder and geopolymer mortars.

Furthermore, in the 970.1 cm^{-1} band, the geopolymer mortar GM0.7 in particular shows the highest intensity. This finding can be explained by the fact that both quartz sand and metakaolin participate in the geopolymerization reaction, which promotes high polycondensation and consequently a strengthening of the cohesion of the geopolymer matrix.

Analysis of the microstructure of the geopolymer binder and mortar by EDS could confirm this reasoning.

3.3.4. Mapping of Chemical Elements

Figure 11 and Figure 12 present the microstructure of the geopolymer binder and a geopolymer mortar respectively, as well as the distribution of oxygen, silicon and aluminum on the surface of these materials. Although the protocol to rigorously study the dissolution of quartz in the geopolymer mortar was not applied,

the following conclusions can be drawn. Figures 11(b)-(d) show a homogeneous distribution of oxygen, silicon and aluminum in the geopolymer binder. This reflects the good dissolution of the calcined clay, which served as a source of aluminosilicates by the alkaline solution. These different chemical elements are the constituents of the geopolymer network, whose monomer is Si-O-Al. On the other hand, the comparison of Figures 12(b)-(d) reveals a higher concentration of silicon compared to that of aluminum within the geopolymer mortar. This seems to indicate the partial dissolution at the surface of the quartz grains, which leads to the increase of siliceous species in the geopolymer matrix mentioned previously in the case of geopolymer mortars.

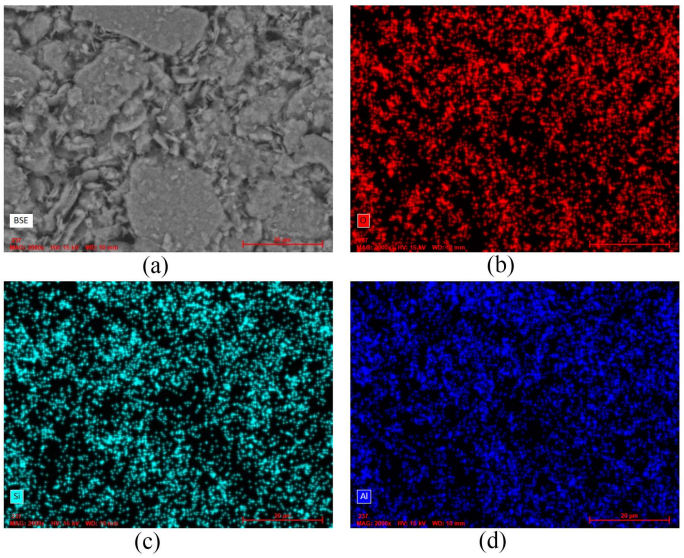

Figure 11. (a) SEM image of the geopolymer binder; (b) EDS of oxygen; (c) EDS of silicon; (d) EDS of aluminum.

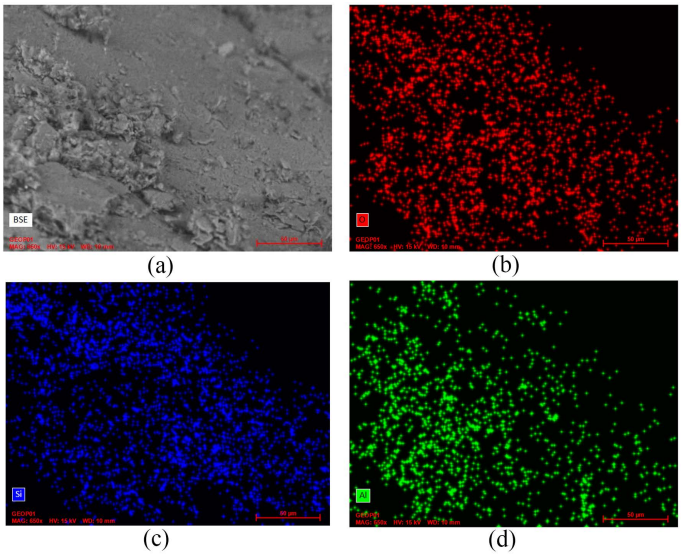

Figure 12. (a) SEM image of geopolymer mortar; (b) EDS of oxygen; (c) EDS of silicon; (d) EDS of aluminum.

Wan *et al.* confirm this reasoning in their study on the reinforcement of metakaolin-based geopolymers with quartz sand. Indeed, it shows from EDS mapping around quartz particles that the Si/Al ratios decrease progressively from the center of the sand grain towards the geopolymer matrix with a certain equality on both sides of the sand grain-geopolymer matrix interface. He therefore concludes that this result indicates the formation of a transitional combination of a few micrometers that transforms the quartz particles into geopolymer gel. This combination therefore seems to be one of the reasons for the increase in the mechanical strength of geopolymer mortars.

4. Conclusions

The study carried out on the influence of sand in the formulation of geopolymer mortars based on metakaolinite has highlighted the important role played by the binder/sand ratio (B/S) on the properties of the geomaterials obtained.

According to the analysis of physical properties, the introduction of sand into the geopolymer binder significantly modified the physical properties of the mortars. These effects were particularly marked for low binder/sand ratios. Indeed, the apparent density increased with the sand content, due to the higher density of sand compared to the pure binder. At the same time, a decrease in the porosity accessible to water was observed with the increase in the amount of sand, thus giving better compactness to the material. The pure binder has a high porosity of 43.18%, while the mortars show reduced values between 16% and 20%, which suggests good durability against environmental aggressions.

Regarding mechanical properties, the results reveal a significant improvement in compressive and flexural strengths following the addition of sand to the geopolymer binder. In particular, for the B/S ratio equal to 0.7 (*i.e.*, 58.8% sand), which appears optimal, the compressive strength reaches 27.09 MPa, which makes it possible to consider structural applications, particularly in the manufacture of blocks for load-bearing and non-load-bearing walls in compliance with NF EN 771-3/CN and Eurocode 6 standards. These mechanical performances, although lower than those of class 32.5 Portland cement mortars, far surpass those of traditional materials such as raw earth bricks or fired bricks.

Microstructure observations (SEM) revealed a geopolymer matrix in which the sand grains are well coated, although discontinuities at the sand-matrix interface exist. This partly explains the relatively low strength values obtained in this study. Mineralogical analysis (XRD) shows that the only mineral phase present in the mortar is quartz due to the addition of sand. This indicates that there is no appearance of new phases, confirming that the microstructure of the mortars consists of an amorphous geopolymer matrix and sand grains. Infrared spectroscopy analysis (FTIR) showed an intensification of the characteristic bands of the Si-O-Si and Si-O-Al bonds, reflecting a more advanced polycondensation in the mortars, particularly for GM0.7. In addition, EDS mapping confirms a good distribution of elements specific to the geopolymeric network (Si, Al, O), with an over-

concentration of silicon reflecting a possible dissolution of the sand. The last two observations would be related to the increase in mechanical resistance up to a certain threshold.

In summary, this study shows that the role of sand is not limited to a simple filler in the geopolymer, but it acts as an active element that participates in the chemical structuring of mortars. The B/S ratio ultimately appears to be the optimal compromise between compactness, chemical reactivity and mechanical performance. The rational use of local sand would make it possible to realize the application of geopolymers in the field of sustainable and ecological construction in tropical areas, particularly in the Ivory Coast.

Conflicts of Interest

The authors declare no conflicts of interest regarding the publication of this paper.

References

[1] Emeruwa, E., Kouadio, K.C., Kouakou, C.H., Boffoué, O.M., Assandé, A.A., Ouattara, S., Coulibaly, Y., Dauscher, A. and Lenoir, B. (2008) Caractérisation des argiles de la région d'Abidjan: Étude comparée de quelques gites et leur perspective de valorisation. *Revue Ivoirienne des Sciences et Technologie*, **11**, 177-192.

[2] Andji, J.Y., Touré, A.A., Kra, G. and Yvon, J. (2009) États d'oxydation du fer dans les kaolins du gisement de Gounioubé: Un outil pour une meilleure compréhension des conditions de formation des kaolinites. *Journal de la Société Ouest-Africaine de Chimie*, **28**, 17-26.

[3] Turner, L.K. and Collins, F.G. (2013) Carbon Dioxide Equivalent (CO_2-e) Emissions: A Comparison between Geopolymer and OPC Cement Concrete. *Construction and Building Materials*, **43**, 125-130. https://doi.org/10.1016/j.conbuildmat.2013.01.023

[4] Nana, A., Alomayri, T.S., Venyite, P., Kaze, R.C., Assaedi, H.S., Nobouassia, C.B., *et al.* (2020) Mechanical Properties and Microstructure of a Metakaolin-Based Inorganic Polymer Mortar Reinforced with Quartz Sand. *Silicon*, **14**, 263-274. https://doi.org/10.1007/s12633-020-00816-4

[5] Burciaga-Diaz, O., Escalante-Garcia, J.I. and Gorokhovsky, A. (2012) Geopolymers Based on a Coarse Low-Purity Kaolin Mineral: Mechanical Strength as a Function of the Chemical Composition and Temperature. *Cement and Concrete Composites*, **34**, 18-24. https://doi.org/10.1016/j.cemconcomp.2011.08.001

[6] Şahin, F., Uysal, M. and Canpolat, O. (2021) Systematic Evaluation of the Aggregate Types and Properties on Metakaolin Based Geopolymer Composites. *Construction and Building Materials*, **278**, Article ID: 122414. https://doi.org/10.1016/j.conbuildmat.2021.122414

[7] Davidovits, J. (1989) Geopolymers and Geopolymeric Materials. *Journal of Thermal Analysis*, **35**, 429-441. https://doi.org/10.1007/bf01904446

[8] Kamarudin, H., Mustafa, Al Bakri A.M., Binhussain, M., Ruzaidi, C.M., Luqman, M., Heah, C.Y. and Liew, Y.M. (2011) Preliminary Study on Effect of NaOH Concentration on Early Age Compressive Strength of Kaolin-Based Green Cement. *International Conference on Chemistry and Chemical Process*, **10**, 18-24.

[9] Yeddula, B.S.R. and Karthiyaini, S. (2020) Experimental Investigations and Prediction of Thermal Behaviour of Ferrosialate-Based Geopolymer Mortars. *Arabian Journal for Science and Engineering*, **45**, 3937-3958.

https://doi.org/10.1007/s13369-019-04314-7

[10] Kong, D.L.Y., Sanjayan, J.G. and Sagoe-Crentsil, K. (2007) Factors Affecting the Performance of Metakaolin Geopolymers Exposed to Elevated Temperatures. *Journal of Materials Science*, **43**, 824-831. https://doi.org/10.1007/s10853-007-2205-6

[11] Liew, Y.M., Kamarudin, H., Bakri, A.M.M.A., Binhussain, M., Luqman, M., Nizar, I.K., *et al.* (2011) Influence of Solids-To-Liquid and Activator Ratios on Calcined Kaolin Cement Powder. *Physics Procedia*, **22**, 312-317. https://doi.org/10.1016/j.phpro.2011.11.049

[12] ASTM International (2013) Standard Guide for Elemental Analysis by Wavelength Dispersive X-Ray Fluorescence Spectrometry. ASTM E1621-13.

[13] AFNOR (2003) Essais non destructifs—Diffraction des rayons X appliquée aux matériaux polycristallins et amorphes—Partie 1: Principes généraux. NF EN 13925-1.

[14] AFNOR (2012) Essais pour déterminer les caractéristiques géométriques des granulats-Partie 1: Détermination de la granularité—Analyse granulométrique par tamisage. NF EN 933-1.

[15] AFNOR (2022) Béton—Essai pour béton durci—Essai de porosité et de masse volumique. NF P18-459.

[16] AFNOR (2016) Méthodes d'essais des ciments—Partie 1: Détermination des résistances. NF EN 196-1.

[17] Singh, S., Aswath, M.U., Das Biswas, R., Ranganath, R.V., Choudhary, H.K., Kumar, R., *et al.* (2019) Role of Iron in the Enhanced Reactivity of Pulverized Red Mud: Analysis by Mössbauer Spectroscopy and FTIR Spectroscopy. *Case Studies in Construction Materials*, **11**, e00266. https://doi.org/10.1016/j.cscm.2019.e00266

[18] Chaabane, L., Moussaceb, K. and Aït-Mokhtar, A. (2018) Efficiency of Stabilization/Solidification of Heavy Metals Contained in Hydroxide Sludge Waste into Metakaolin Based Geopolymers. *Environmental Progress & Sustainable Energy*, **38**, Article ID: 13137. https://doi.org/10.1002/ep.13137

[19] Bich, C. (2005) Contribution à l'étude de l'activation thermique du kaolin: Évolution de la structure cristallographique et activité pouzzolanique. Master's Thesis, Institut National des Sciences Appliquées de Lyon.

[20] Benalia, S., Zeghichi, L. and Benghazi, Z. (2022) A Comparative Study of Metakaolin/Slag-Based Geopolymer Mortars Incorporating Natural and Recycled Sands. *Civil Engineering Journal*, **8**, 1622-1638. https://doi.org/10.28991/cej-2022-08-08-07

[21] Das, B.M. and Sobhan, K. (2018) Principles of Geotechnical Engineering. Cengage Learning.

[22] Kuenzel, C., Li, L., Vandeperre, L., Boccaccini, A.R. and Cheeseman, C.R. (2014) Influence of Sand on the Mechanical Properties of Metakaolin Geopolymers. *Construction and Building Materials*, **66**, 442-446. https://doi.org/10.1016/j.conbuildmat.2014.05.058

[23] Ferone, C., Liguori, B., Capasso, I., Colangelo, F., Cioffi, R., Cappelletto, E., *et al.* (2015) Thermally Treated Clay Sediments as Geopolymer Source Material. *Applied Clay Science*, **107**, 195-204. https://doi.org/10.1016/j.clay.2015.01.027

[24] AFNOR (2012) Spécification pour éléments de maçonnerie—Partie 3: Éléments de maçonnerie en béton de granulats (granulats courants et légers)—Complément national à la NF EN 771-3:2011. NF EN 771-3/CN.

[25] AFNOR (2022) Briques et Blocs de terre crue pour murs et cloisons—Définitions—Spécifications—Méthodes d'essai—Conditions de réception. XP P 13-901.

[26] AFNOR (2006) Eurocode 6—Calcul des ouvrages en maçonnerie—Partie 1-1: Règles

communes pour ouvrages en maçonnerie armée et non armée. Eurocode 6 NF EN 1996-1-1.

[27] Wan, Q., Rao, F., Song, S., Cholico-González, D.F. and Ortiz, N.L. (2017) Combination Formation in the Reinforcement of Metakaolin Geopolymers with Quartz Sand. *Cement and Concrete Composites*, **80**, 115-122. https://doi.org/10.1016/j.cemconcomp.2017.03.005

[28] Jaya, N.A., Liew, Y.M., Heah, C.Y. and Abdullah, M.M.A.B. (2018) Effect of Solid-To-Liquid Ratios on Metakaolin Geopolymers. *AIP Conference Proceedings*, **2045**, Article ID: 020099. https://doi.org/10.1063/1.5080912

[29] Henon, J. (2012) Élaboration de matériaux poreux géopolymères à porosité multi-échelle et contrôlée. Master's Thesis, Université de Limoges.

[30] Luukkonen, T., Sarkkinen, M., Kemppainen, K., Rämö, J. and Lassi, U. (2016) Metakaolin Geopolymer Characterization and Application for Ammonium Removal from Model Solutions and Landfill Leachate. *Applied Clay Science*, **119**, 266-276. https://doi.org/10.1016/j.clay.2015.10.027

[31] Zhang, M., Zhao, M., Zhang, G., El-Korchi, T. and Tao, M. (2017) A Multiscale Investigation of Reaction Kinetics, Phase Formation, and Mechanical Properties of Metakaolin Geopolymers. *Cement and Concrete Composites*, **78**, 21-32. https://doi.org/10.1016/j.cemconcomp.2016.12.010

[32] Lucas, S., Tognonvi, M.T., Soro, J., Rossignol, S. and Gelet, J.L. (2010) Consolidation of Sand by Alkaline Silicate Solution. *Advances in Science and Technology*, **68**, 84-89. https://doi.org/10.4028/www.scientific.net/ast.68.84

[33] Niibori, Y., Kunita, M., Tochiyama, O. and Chida, T. (2000) Dissolution Rates of Amorphous Silica in Highly Alkaline Solution. *Journal of Nuclear Science and Technology*, **37**, 349-357. https://doi.org/10.1080/18811248.2000.9714905